# Core requirements for *glmS* ribozyme self-cleavage reveal a putative pseudoknot structure

Garrett A. Soukup*

Department of Biomedical Sciences, Creighton University School of Medicine, 2500 California Plaza, Omaha, NE 68178, USA

## ABSTRACT

The *glmS* ribozyme is a self-cleaving RNA catalyst that resides in the 5′-untranslated region of *glmS* mRNA in certain bacteria. The ribozyme is specifically activated by glucosamine-6-phosphate (GlcN6P), the metabolic product of the GlmS protein, and is thus proposed to provide a feedback mechanism of riboswitch regulation. Both phylogenetic and biochemical analyses of the *glmS* ribozyme have established a highly conserved core sequence and secondary structure required for GlcN6P-dependent self-cleavage. However, the high degree of nucleotide conservation offers few clues regarding the higher-order structural organization of the catalytic core. To further investigate core ribozyme structure, minimal 'consensus-type' *glmS* ribozymes that retain GlcN6P-dependent activity were produced. Mutational analyses of consensus-type *glmS* ribozymes support a model for core ribozyme folding through a pseudoknot structure formed by the interaction of two highly conserved sequence segments. Moreover, GlcN6P-dependent function is demonstrated for bimolecular constructs in which substrate interaction with the ribozyme is minimally comprised of sequence representing that involved in putative pseudoknot formation. These studies suggest that the *glmS* ribozyme adopts an intricate multi-strand catalytic core through the formation of a pseudoknot structure, and provide a refined model for further considering GlcN6P interaction and GlcN6P-dependent ribozyme function.

## INTRODUCTION

Riboswitches are genetic regulatory elements within RNA transcripts that modulate gene expression in response to direct interactions with metabolites. For the nine classes of bacterial riboswitches that respond to adenosylcobalamin, thiamine pyrophosphate, flavin mononucleotide, *S*-adenosylmethionine, guanine, adenine, lysine and glycine, gene expression is affected by metabolite-dependent regulation of either transcription termination or translation initiation (1–3). The presence of thymine pyrophosphate-binding domains in eukaryotic introns and 3′-untranslated regions (3′-UTRs) suggests riboswitches might additionally function by regulating RNA processing (4). Moreover, recent studies have identified the *glmS* ribozyme, a metabolite-dependent self-cleaving RNA catalyst, as a unique member of the riboswitch family (5,6).

The *glmS* ribozyme resides in the 5′-UTR of *glmS* mRNA in at least 18 gram positive bacteria including *Bacillus subtilis*, *Bacillus cereus* and *Bacillus anthracis* (5,6). The ribozyme is specifically activated by glucosamine-6-phosphate (GlcN6P) (5), the metabolic product of GlcN6P synthase encoded by *glmS*. Thus, the *glmS* ribozyme likely provides a feedback mechanism for regulating GlcN6P synthase and GlcN6P production. Accordingly, mutations that disrupt *glmS* ribozyme self-cleavage have been demonstrated to derepress reporter gene expression *in vivo* (5), suggesting that ribozyme activity promotes mRNA decay and/or prevents translation.

Phylogenetic and biochemical analysis of the *glmS* ribozyme reveal that the RNA catalyst is composed of four paired regions (P1–P4) containing or adjoined by highly conserved sequence segments (5,6). Importantly, segments adjacent to and including P1 and P2 constitute the catalytic core to which GlcN6P-dependent self-cleavage activity is attributable (Figure 1A), whereas the P3 and P4 domains are dispensable but function to enhance ligand-dependent catalysis (5). Self-cleavage occurs at the 5′ end of the highly conserved catalytic core resulting in products that possess 2′,3′-cylic phosphodiester and 5′-hydroxyl termini (5). Therefore, the *glmS* ribozyme catalyzes an internal phosphoester transfer reaction identical to other self-cleaving RNA catalysts including the hammerhead, hairpin, hepatitis delta virus and *Neurospora* Varkud satellite (VS) ribozymes (7,8). Additionally, *glmS* ribozymes exhibit comparable rates of self-cleavage in the range of 1–3 $min^{-1}$ (5,9). However, the *glmS* ribozyme
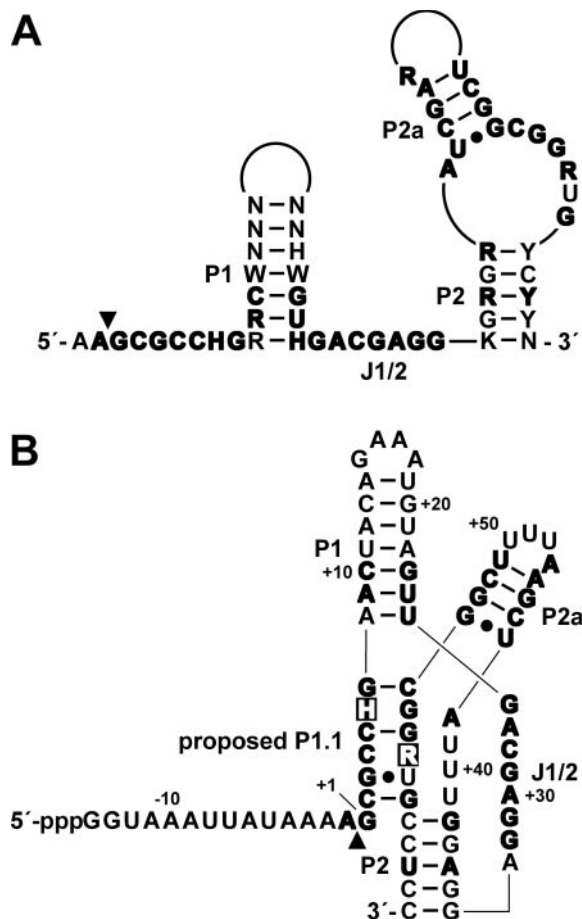
**Figure 1.** Minimal *glmS* ribozyme core. (**A**) Consensus sequence. Nucleotides that are >80% and >90% conserved among an 18-member phylogeny (6) are depicted in plain and bold type, respectively. Short thick lines represent base-pairing interactions that are >80% conserved, whereas longer thick lines indicate regions of variable length and sequence. The cleavage site is denoted by an arrowhead. H = A,C,U; K = G,U; N = G,A,C,U; R = A,G; and W = A,U. (**B**) Consensus-type ribozyme construct. Depicted is the proposed P1.1 interaction and pseudoknot organization of ribozyme constructs based on the consensus sequence. Thin lines bridge contiguous sequence, and nucleotides are numbered relative to the cleavage site (arrowhead). Phylogenetically variable positions H6 and R58 within P1.1 are highlighted.

is mechanistically unique in that self-cleavage activity is absolutely dependent upon GlcN6P or related amine-containing compounds (9), suggesting that ligand might function as a coenzyme in catalysis.

The secondary structure model for the *glmS* ribozyme core provides little indication regarding the organization of highly conserved sequence elements that are likely to form the ligand-binding and catalytic sites. Like other self-cleaving RNA catalysts, the *glmS* ribozyme must structurally incorporate the cleavage site within the catalytic core to effect catalysis. Thus, the conserved sequence segment intervening the cleavage site and P1 presumably interacts with other conserved sequence segments through Watson–Crick and/or non-canonical base-pairing interactions to organize the catalytic core of the ribozyme. While covariant nucleotide identities in the phylogeny of *glmS* ribozymes strongly support both P1 and P2 (6), the strict conservation of nucleotide identities in the remaining sequence segments precludes

phylogenetic evidence for additional secondary or tertiary structural organization of the catalytic core. It is interesting to note, however, that a fair degree of complementarity exists between the conserved sequence segment preceding P1 and that comprising the 3′ asymmetric internal loop between P2 and the region predicted to form P2a. The proposed interaction of these sequence segments forming P1.1 constitutes a pseudoknot structure that would effectively organize the *glmS* ribozyme core (e.g. Figure 1B), thus bringing together in 3D proximity each highly conserved sequence segment and the cleavage site.

In this study, the proposed P1.1 interaction is examined using a series of 'consensus-type' *glmS* ribozymes to facilitate analyses (Figure 1B). Mutational analyses of phylogenetically variable and invariant positions within the proposed P1.1 interaction demonstrate that GlcN6P-dependent self-cleavage activity is consistent with P1.1 formation. Furthermore, metabolite-dependent function is demonstrated for bimolecular constructs that reconstitute the *glmS* ribozyme core solely through sequence representing the proposed P1.1 interaction.

## MATERIALS AND METHODS

### Preparation of constructs

Double-stranded DNA templates for transcription of each self-cleaving ribozyme construct were prepared from synthetic DNA. Templates for construct 1 were prepared by annealing primers 5′-TAATACGACTCACTATAGGTAAATTATAA-AAGCGCCAGAACTACAGAAATGTAGTTGACGAGGAG and 5′-GGAGGCATCCGCCGAAAATTCGATAAACCTCC-TCCTCGTCAACTACATTTC, followed by extension using SuperScript II reverse transcriptase (Invitrogen). Templates for constructs 2–24 were similarly prepared from oligonucleotides containing appropriate substitutions at positions within each segment corresponding to the proposed P1.1 interaction (underlined). Templates for transcription of *trans*-cleaving ribozyme constructs 3t and 4t were similarly prepared by replacing the former primer with 5′-TAATACGACTCACTATAGGAACTA-CAGAAATGTAGTTGACGAGGAG. Template for the *B.cereus trans*-cleaving ribozyme construct (Bce-t) was similarly prepared from primers 5′-TAATACGACTCACTATAGGAAC-TACAAGTAGTGTAGTTGACGAGGTG and 5′-TGCGGTT-GTGATGAACAACCGGGAGCCATCCGCCGAAATCTC-GATAAACCCCACCTCGTCAACTACACTA.

Each construct was transcribed using T7 RNA polymerase and purified by denaturing (8 M urea) 10% PAGE. Self-cleaving ribozyme constructs were internally $^{32}$P-labeled by addition of $[\alpha\text{-}^{32}\text{P}]$UTP to transcription reactions, and quantified using a scintillation counter. Unlabeled *trans*-cleaving ribozyme constructs were quantified by UV spectrophotometry.

### Self-cleavage reactions

Radiolabeled ribozyme (<1 μM) was reacted at 23°C under standard conditions [50 mM Tris–HCl (pH 7.5 at 23°C), 20 mM MgCl$_2$ and 1 mM GlcN6P] or as otherwise noted in each figure legend. Reactions were terminated by the addition of an equal volume of gel loading buffer containing 10 M urea

and 20 mM EDTA. Products were separated by denaturing 10% PAGE and analyzed using a PhosphorImager and IMAGEQUANT software (Molecular Dynamics). Observed rate constants ($k_{obs}$) for self-cleavage were derived by plotting the natural logarithm of the fraction of uncleaved RNA versus time and establishing the negative slope of the resulting line. Stated values represent the average of two replicate assays. The apparent dissociation constant ($K_d$) was established as the concentration of GlcN6P required to produce a half-maximal $k_{obs}$ value.

### *Trans*-cleavage reactions

Synthetic RNA substrate (5′-AAAGCGCCUG) was 5′-$^{32}$P end-labeled using T4 polynucleotide kinase (Invitrogen) and [γ-$^{32}$P]ATP, and purified by denaturing 20% PAGE. Single turnover reactions were performed by incubating unlabeled ribozyme (10 nM to 10 μM) with trace (<10 nM) labeled substrate under standard conditions containing 10 mM GlcN6P. Reactions were terminated, and products were separated by denaturing 20% PAGE and analyzed as described for self-cleavage reactions. The apparent Michaelis–Menten constant ($K_M$) was established as the concentration of ribozyme required to produce a half-maximal $k_{obs}$ value.

## RESULTS

### Characterization of a consensus-type *glmS* ribozyme

In order to best assess phylogenetic differences in the proposed P1.1 interaction, a series of 'consensus-type' *glmS* ribozymes were constructed to provide a homogeneous framework with regard to other features of the catalyst (Figure 1B). The consensus-type ribozymes incorporate every core primary and secondary sequence element that is 80–100% conserved among each member of the *glmS* ribozyme phylogeny. Regions of variable length and sequence are 'generically' rendered and include (i) a GAAA tetraloop as the terminal loop of P1 demonstrated to maintain functionality of the *B.subtilis glmS* ribozyme (5), (ii) poly(U) segments within the terminal loop of P2a and 5′-internal loop between P2 and P2a that are common among *glmS* ribozymes, (iii) an adenosine (A33) at the 3′ end of J1/2 that is common among the majority (but <80%) of *glmS* ribozymes, and (iv) an A-U rich segment 5′ relative to the cleavage site similar to that of the *B.cereus glmS* ribozyme. Sequences comprising P1 and P2 are identical to those of the *B.cereus* and *B.subtilis glmS* ribozymes, respectively. Each consensus-type ribozyme thus possesses an otherwise common architecture in which to assess the phylogenetically variable H6 and R58 positions within the proposed P1.1 interaction (Figure 1B).

To demonstrate functionality, the activity of one consensus-type ribozyme containing A6 and A58 (construct 1) was examined in detail. Construct 1 exhibits GlcN6P-dependent self-cleavage activity (Figure 2A) that is enhanced ∼1000-fold in the presence of ligand to provide an observed rate constant ($k_{obs}$) of 0.2 min$^{-1}$ (Figure 2B). The activity of construct 1 is therefore comparable with that of the full-length *B.subtilis* and *B.cereus glmS* ribozymes (5,9) despite
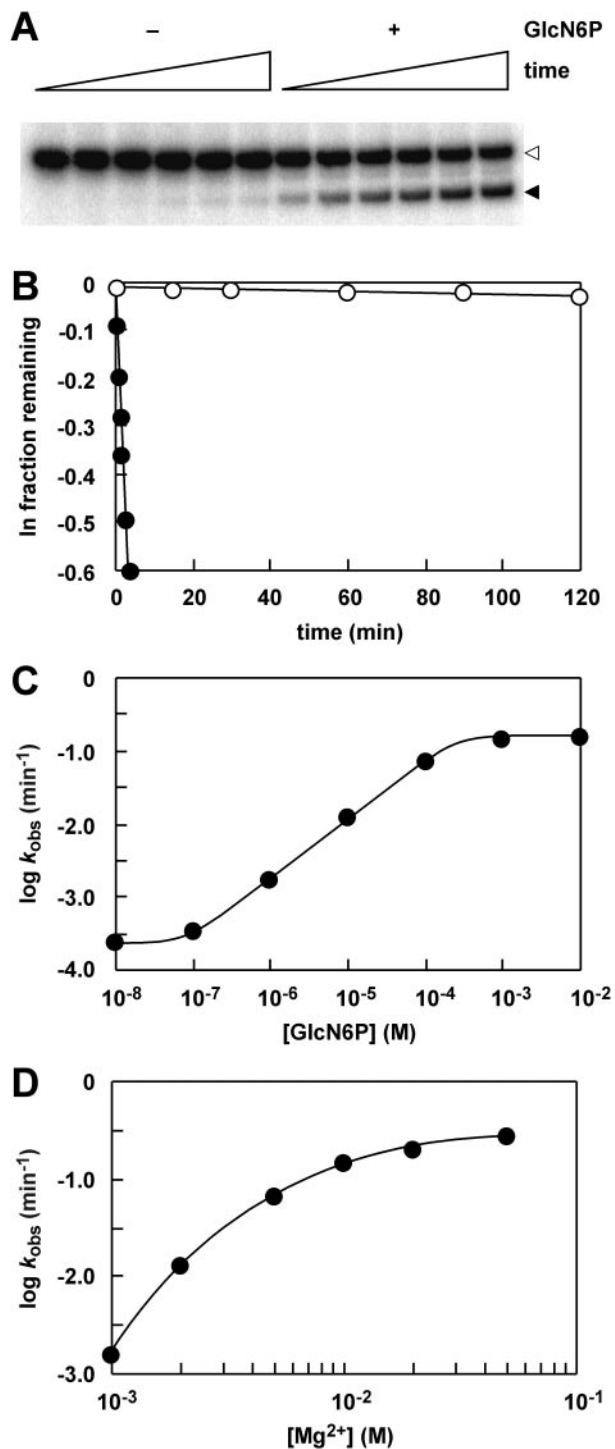


**Figure 2.** Characterization of a consensus-type ribozyme containing A6 and A58 (construct 1). (**A**) GlcN6P-dependent self-cleavage activity. Reactions were incubated between 1 and 120 min in the absence of GlcN6P (−) or between 0.5 and 4 min in the presence of GlcN6P (+), and products were separated on a denaturing 10% polyacrylamide gel. Open and closed arrowheads indicate precursor ribozyme and its 3′-cleavage product, respectively. (**B**) Rate of self-cleavage in the absence (open circles) or presence (closed circles) of GlcN6P. (**C**) Dependence of rate on GlcN6P concentration. The concentration of GlcN6P corresponding to a half-maximal rate constant for self-cleavage indicates the apparent $K_d$ for ligand to be ∼200 μM. (**D**) Dependence of rate on magnesium ion concentration. All reactions were performed under standard conditions except where GlcN6P or MgCl$_2$ concentration was varied.
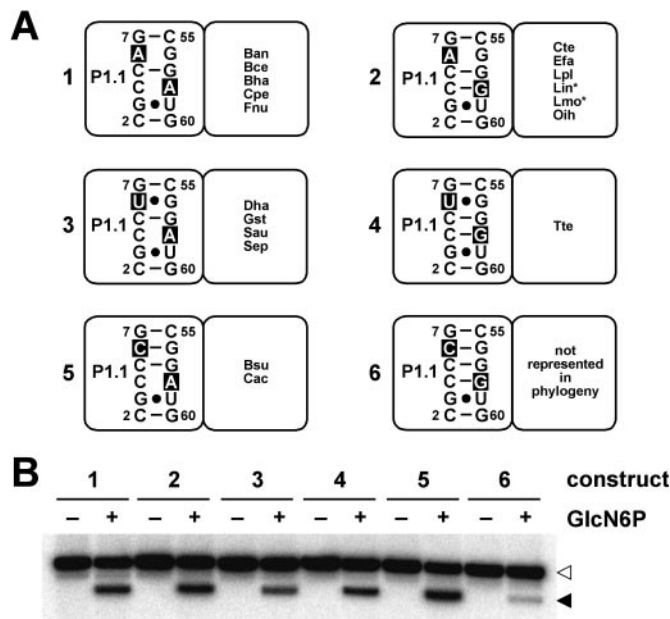
**Figure 3.** Impact of nucleotide identities at positions H6 and R58 on consensus-type ribozyme activity. (**A**) Six possible ribozyme constructs and their representation by organism within the 18-member phylogeny of *glmS* ribozymes. Depicted is the proposed P1.1 interaction alone for each construct in the same orientation as shown in Figure 1B, where the H6 and R58 positions are highlighted. Asterisks indicate organisms in which the ribozyme additionally contains a U59A substitution. Abbreviations for each organism are as described previously (6). (**B**) GlcN6P-dependent self-cleavage activities of constructs 1 through 6. Ribozymes were reacted for 2 min under standard conditions except where GlcN6P was omitted, and products were resolved as described in the legend to Figure 2.

an approximate order of magnitude reduction in $k_{obs}$ likely attributable to deletion of the P3 and P4 domains. Further analysis of the activity of construct 1 in the presence of various concentrations of GlcN6P demonstrates the apparent dissociation constant ($K_d$) for GlcN6P to be $\sim$200 µM (Figure 2C). This value is identical to that determined previously for the full-length *B.subtilis glmS* ribozyme (5), suggesting that the P3 and P4 domains have little or no impact upon GlcN6P recognition or binding affinity. Similar analysis of construct 1 with various concentrations of magnesium chloride shows a relative increase in dependence upon magnesium ions compared with the full-length *B.subtilis glmS* ribozyme (5). These data suggest that P3 and P4 are peripheral domains that in part enhance catalysis by reducing the metal ion dependence of the catalytic core. Taken together, results for construct 1 demonstrate that the 'generically' rendered consensus-type ribozyme provides a functional architecture within which P1.1 formation can be further examined. Therefore, no optimization of the consensus-type platform was attempted or deemed necessary.

## Combinatorial analysis of variable positions in P1.1

Considering the two variable positions H6 and R58 within the conserved sequence segments that comprise the proposed P1.1 interaction (Figure 1B), there are six combinatorial configurations (Figure 3A). Among the eighteen *glmS* ribozymes found in nature, 5 of the 6 possible combinations for nucleotides corresponding to H6 and R58 are represented

(Figure 3A). Importantly, consensus-type ribozymes enable an analysis of variations at these positions in an otherwise homogeneous context. In addition to construct 1, which is representative of five phylogenetic members, five additional constructs (2 through 6) representing the remaining combinations for H6 and R58 were prepared (Figure 3A). A direct comparison of GlcN6P-dependent self-cleavage activities of constructs 1 through 6 demonstrates that each combination of H6 and R58 represented by naturally occurring *glmS* ribozymes (constructs 1 through 5) enables similar catalytic activity in relatively short (2 min) reactions (Figure 3B). These data suggest that natural variation of H6 and R58 does not necessarily occur in compensation for variations at other positions in each phylogenetic member, as they are absent from consensus-type ribozymes. However, such a result is expected on the basis that variations at H6 and R58 affect mainly only P1.1 formation.

Most variations at H6 and R58 increase the helical character of the proposed P1.1 interaction compared with construct 1. Of the five combinations represented by naturally occurring *glmS* ribozymes, construct 4 containing U6 and G58 (Figure 3A) possesses the greatest predicted thermodynamic stability for P1.1 based on the number of base pairs and G–C content. Notably, the U6 and G58 combination is represented by corresponding nucleotide identities within the *glmS* ribozyme from *Thermoanaerobacter tengcongensis*, an extreme thermophile isolated from a freshwater hot spring (10,11). Possibly, the greater predicted stability of the proposed P1.1 interaction afforded by U6 and G58 could be a component that benefits *glmS* ribozyme function at elevated temperatures. Interestingly, the unrepresented combination of C6 and G58 in construct 6 possesses a greater helical character and predicted thermodynamic stability for P1.1 (Figure 3A). However, the combination is a relative detriment to GlcN6P-dependent self-cleavage activity (Figure 3B), as other constructs exhibit 4- to 8-fold greater self-cleavage activities. This observation is consistent with the fact that the C6 and G58 combination is not represented by corresponding nucleotides in the phylogeny of *glmS* ribozymes, and suggests that uniform helicity of the proposed P1.1 interaction perturbs other interactions that contribute to ribozyme activity.

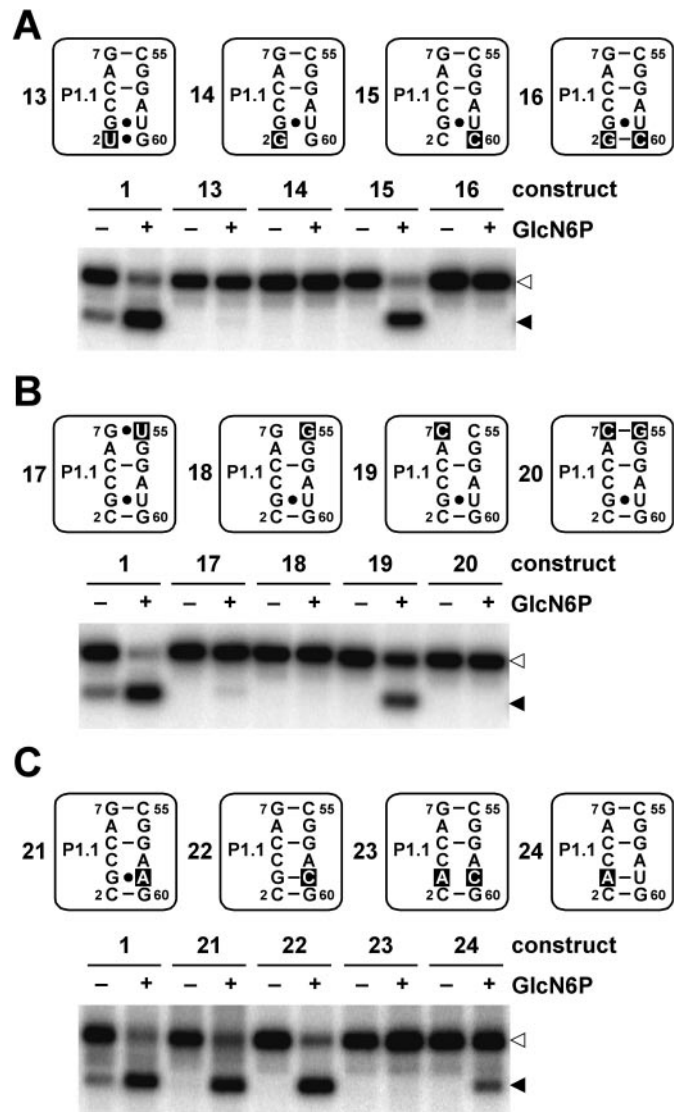## Mutational analysis of invariant positions in P1.1

In order to provide evidence for individual base-pairing interactions in the proposed P1.1 helix, mutational analyses of phylogenetically invariant positions were performed. Although mutation of conserved nucleotides is expected to disrupt ribozyme activity for any number of reasons, compensatory mutations that substitute proposed base-pairing interactions might partially restore self-cleavage activity dependent upon the importance of other interactions that remain disrupted. Thus, each of the four proposed base-pairing interactions in P1.1 of construct 1 were scrutinized by examining the catalytic activities of mutant constructs in relatively long (20 h) reactions.

For the C5–G57 proposed base-pairing interaction in P1.1, the activities of six single- or double-mutant constructs relative to construct 1 were examined (Figure 4A). Constructs containing either C5G or G57C mutations alone (constructs 7 and 8, respectively) or in combination (construct 9) were
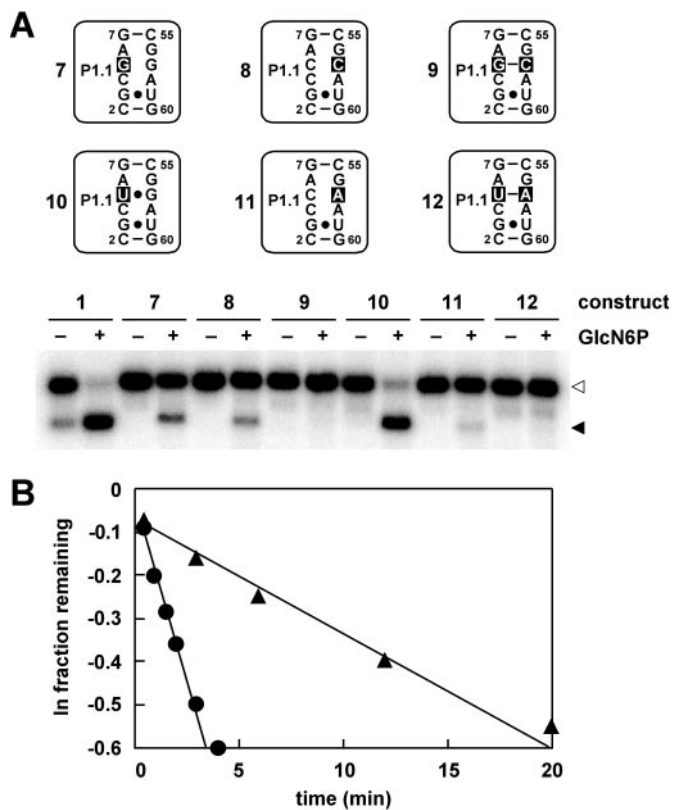
**Figure 4.** Mutational analysis of conserved positions comprising the C5–G57 base pair in the putative P1.1 interaction. (**A**) Activity of six ribozyme construct designed to disrupt or maintain base pairing. Depicted is the proposed P1.1 interaction alone for each construct in the same orientation as shown in Figure 1B, where mutations relative to construct 1 are highlighted. Also shown are the GlcN6P-dependent self-cleavage activities of constructs 1 and 7–12 under standard conditions for 20 h as otherwise described in the legend to Figure 2. (**B**) Rate of self-cleavage in the presence of GlcN6P for constructs 1 (circles) and 7 (triangles) under standard conditions.



**Figure 5.** Mutational analysis of conserved positions comprising terminal base pairs in the putative P1.1 interaction. (**A**) Mutational analysis of conserved C2 and G60 positions. (**B**) Mutational analysis of conserved G7 and C55 positions. (**C**) Mutational analysis of conserved G3 and U59 positions. Each construct depicts the proposed P1.1 interaction alone in the same orientation as shown in Figure 1B, where mutations relative to construct 1 are highlighted. Depicted are the GlcN6P-dependent self-cleavage activities of constructs 1 and 13–16, 17–20 or 21–24 under standard conditions for 20 h as otherwise described in the legend to Figure 2.

examined to determine the effect of disrupting or substituting the proposed base-pairing interaction. Constructs 7 and 8 exhibit weak GlcN6P-dependent activity, demonstrating that mutation of either conserved nucleotide or disruption of the proposed base pairing is largely detrimental to activity. Construct 9 possesses no detectible activity, showing that the alternate pairing or the cumulative effects of both mutations is entirely detrimental. Additional constructs containing either C5U or G57A mutations alone (constructs 10 and 11) or in combination (construct 12) similarly demonstrate that disrupting or substituting the proposed pairing results in weak or undetectable activity (constructs 11 and 12, respectively). However, the C5U mutation (construct 10), which does not preclude the formation of a U5•G57 base pair, has little effect on GlcN6P-dependent self-cleavage activity. Further analysis of construct 10 demonstrates that the C5U mutation results in less than an order of magnitude loss of ribozyme activity compared with construct 1 (Figure 4B). Despite the relatively modest effect of the C5U mutation on the activity of the *glmS* ribozyme core, cytidine identity of the corresponding nucleotide in the phylogeny of *glmS* ribozymes is absolutely conserved and suggests that optimal activity is required for biological function. These data demonstrate, that G57 in

particular is requisite for ribozyme reactivity, and provide only modest evidence for C5–G57 pairing in the proposed P1.1 interaction.

The two terminal base-pairing interactions in the proposed P1.1 helix were similarly examined (Figure 5A and B). For the proposed C2–G60 base pair, C2U (construct 13) or C2G (construct 14) mutations are detrimental to ribozyme activity whereas G60C (construct 15) has relatively little effect (Figure 5A). These data demonstrate that C2 more so than G60 is requisite for ribozyme activity and provide an explanation for the lack of activity observed for constructs containing alternate U2•G60 (construct 13) and G2–C60 (construct 16) pairings. For the proposed G7–C55 base pair, C55U

(construct 17) or C55G (construct 18) mutations are detrimental to ribozyme activity whereas G7C (construct 19) has a much less profound effect (Figure 5B). These data similarly demonstrate that C55 more so than G7 is requisite for ribozyme activity and explain the lack of activity for constructs containing alternate G7•U55 (construct 17) and C7–G55 (construct 20) pairings. Consequently, the apparent strict requirement for C2 and C55 preclude the possibility of providing evidence for the terminal base pairs of the proposed P1.1 interaction in this mutational analysis.

For the proposed G3•U59 base-pairing interaction, phylogenetic data indicate that pairing might be more adaptable. Two members of the *glmS* ribozyme phylogeny contain adenosine at the corresponding U59 position (6), suggesting that U59A should be an allowable substitution. Indeed, U59A mutation (construct 21) has relatively little effect on core ribozyme activity, supporting the probability of G3•A59 base pairing (Figure 5C). Following this line of reasoning, U59C mutation, which is not represented in the *glmS* ribozyme phylogeny, should also support GlcN6P-dependent self-cleavage activity. Accordingly, U59C mutation (construct 22) similarly maintains ribozyme activity, consistent with the possibility of G3–C59 pairing (Figure 5C). These data demonstrate that although U59 is highly conserved, the nucleotide identity is largely adaptable presuming that base pairing is maintained. Therefore, the possibility of G3–C59 pairing was disrupted by an additional G3A mutation (construct 23) and restored to an alternate A3–U59 pairing (construct 24). Importantly, construct 23 is devoid of activity while construct 24 restores GlcN6P-dependent self-cleavage activity, albeit weak. These data demonstrate that G3 is an important feature of the *glmS* ribozyme core and that position 59 appears adaptable as long as it maintains base-pairing potential within the proposed P1.1 helix. Arguably, the putative G•A pair (construct 21) is better accommodated in a helical conformation than certain other mismatches. Dependent upon context, G•A pairing can have little effect on model helix stability (12) and is found in many helical RNA structures (13). Mutational analyses, in so far as they can be applied to these highly conserved sequence domains, are therefore consistent with two of the four base-pairing interactions in the P1.1 helix and thus provide modest support for the putative pseudoknot structure of the *glmS* ribozyme core.

## Analysis of bimolecular ribozyme constructs

The putative pseudoknot organization of the *glmS* ribozyme core predicts that the catalyst can be reconstructed from two RNA fragments through any of the base-pairing interactions that compose the core structure. Indeed, one such bimolecular construct has been demonstrated to reconstitute GlcN6P-dependent activity when 'substrate' and 'ribozyme' fragments are brought together mainly by P1 formation (6). However, to examine whether P1.1 formation alone is sufficient to reconstruct the core ribozyme and reconstitute GlcN6P-dependent activity, the consensus-type ribozymes represented by constructs 3 and 4 were split into substrate and ribozyme fragments at the proposed P1.1 and P1 junction (Figure 6A). Thus, substrate is minimally represented by a synthetic RNA decamer that might form P1.1 with *trans*-acting ribozyme constructs (constructs 3t and 4t). It is important to note,
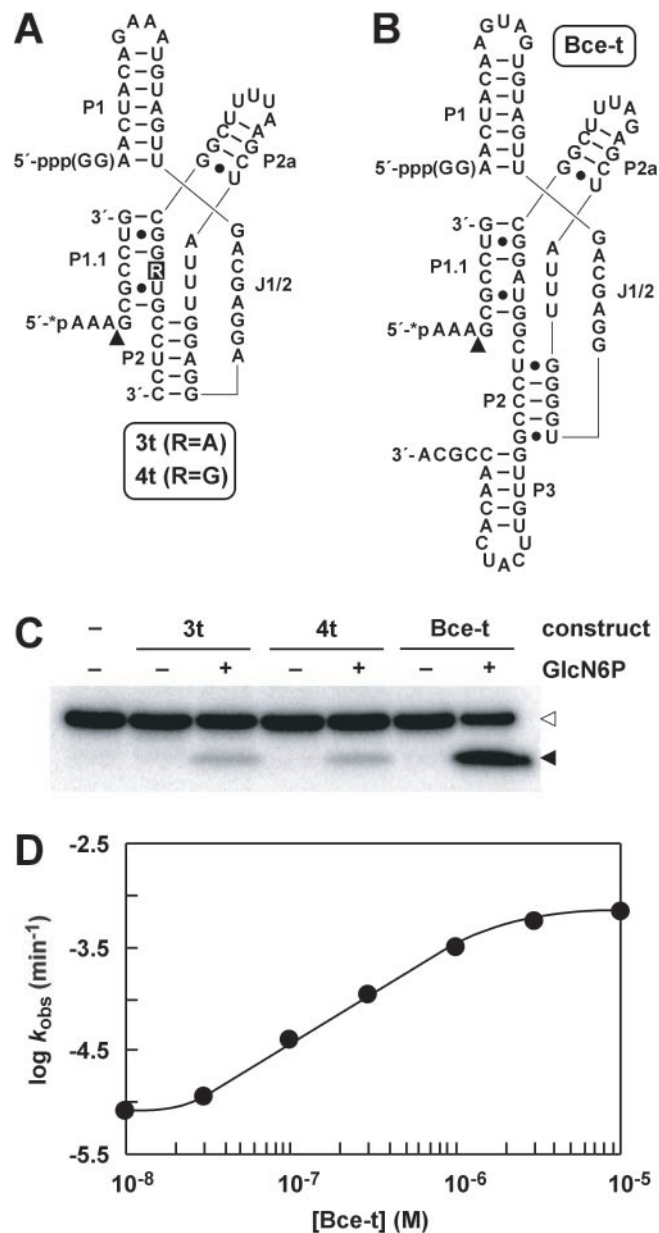


**Figure 6.** *Trans*-cleavage of a substrate that reconstitutes the putative P1.1 interaction. (**A**) Design of *trans*-cleaving ribozymes derivative of constructs 3 and 4 (3t and 4t, respectively). (**B**) Design of a *trans*-cleaving construct derivative of the *B.cereus glmS* ribozyme (Bce-t). Guanosines shown in parentheses at the 5′ end of each *trans*-cleaving ribozyme construct were introduced to facility *in vitro* transcription. Asterisks denote end-labeled substrate. (**C**) *Trans*-cleavage of substrate. Depicted is the activity of each construct in the absence or presence of 10 mM GlcN6P under standard conditions for 20 h. Products were separated on a denaturing 20% polyacrylamide gel. Open and closed arrowheads indicate the substrate and its 5′-cleavage product, respectively. (**D**) Dependence of rate on Bce-t concentration. Rate constants at various ribozyme concentrations were determined under standard conditions containing 10 mM GlcN6P. The concentration of ribozyme corresponding to a half-maximal rate constant for *trans*-cleavage indicates the apparent $K_M$ for substrate to be ∼1 μM.

however, that such bimolecular reconstruction of the core ribozyme does not restore the conformational constraint imposed by pseudoknot formation, and therefore is expected to significantly impair ribozyme activity.

Analysis of bimolecular ribozyme function indeed demonstrates that constructs 3t and 4t are capable of reconstituting GlcN6P-dependent activity with a short end-labeled RNA substrate (Figure 6C). In this analysis, the proposed P1.1 interaction differs only by the absence or presence of a predicted base pairing with R58 between constructs 3t and 4t, respectively, but has no perceivable effect on substrate cleavage. Expectedly, GlcN6P-dependent substrate cleavage by constructs 3t and 4t is weak, likely owing to a loss of conformational constraint in the consensus-type ribozyme core. Considering that consensus-type ribozymes represent an 'averaged' rather than optimal *glmS* ribozyme core structure, substrate interaction and cleavage using a *trans*-acting construct derivative of the *B.cereus glmS* ribozyme (Bce-t; Figure 6B) was examined. The Bce-t construct exhibits markedly enhanced GlcN6P-dependent substrate interaction and cleavage (Figure 6C), suggesting relatively improved organization or activity of the natural ribozyme core. Further analysis of substrate interaction and cleavage using the Bce-t construct demonstrates a dependence of cleavage activity upon *trans*-acting ribozyme concentration that is saturable (Figure 6D), providing an apparent $K_M$ value of $\sim$1 µM. These data therefore demonstrate that the conserved sequence segment 5$'$ relative to P1 possesses a mode of interaction with the remaining *glmS* ribozyme core that is consistent with the proposed P1.1 interaction.

## DISCUSSION

The proposed P1.1 interaction and consequent pseudoknot structure for the *glmS* ribozyme core provide a plausible tertiary architecture for the self-cleaving catalyst that brings the cleavage site and conserved secondary structure elements into 3D proximity. The P1 and P2 domains might thus form a compact, multi-strand active site that is both capable of binding GlcN6P and promoting transesterification. The P1.1 interaction is supported by mutational analyses of phylogenetically variable and invariant positions in an otherwise homogenous context of consensus-type ribozymes. Results demonstrate that two of the four proposed base pairs can be substituted by non-natural base-pairing interactions only in so far as strong sequence requirements permit. Dependent upon the identity of variable positions, the P1.1 interaction might be comprised by as many as six contiguous base pairs including canonical Watson–Crick and non-canonical pairs. Moreover, bimolecular constructs demonstrate that active *glmS* ribozyme cores can be reconstituted by the intermolecular interaction of substrate and ribozyme RNAs through none other than the sequences representing the P1.1 interaction. Although bimolecular constructs exhibit a substantial loss of activity that is likely attributable to the loss of conformational restraint that would be imposed by the pseudoknot, the interaction of ribozyme with substrate demonstrates an apparent $K_M$ of $\sim$1 µM. By comparison, intermolecular interaction of a substrate RNA with the group I ribozyme through the formation of a 6 bp P1 helix exhibits a $K_M$ of 50 nM (14). Therefore, the intermolecular P1.1 interaction is consistent with that expected for a relatively thermodynamically destabilized helix.

It is interesting to note the pattern of conservation and demonstrated importance of nucleotide identities within the proposed P1.1 interaction. Specifically, C2, G3 and C4 are absolutely conserved, and mutations at these positions are relatively more detrimental to ribozyme activity than are their juxtaposed partners G60, U59 and R58, respectively. Similarly, C55, G56 and G57 are absolutely conserved, and mutations at these positions are relatively more detrimental to ribozyme activity than are their juxtaposed partners G7, H6 and C5, respectively. Thus, it appears that nucleotides most accessible upon one face of the proposed P1.1 helix underlie ribozyme activity in a relatively more meaningful way. Possibly, these nucleotides mediate tertiary interactions with other conserved elements of the *glmS* ribozyme core such as the J1/2 segment to establish complex ligand-binding and/or active sites. This interpretation is reminiscent of P1 helix recognition in the group I ribozyme by other conserved sequence segments (15).

The proposed P1.1 helix represents one of two pseudoknots in the *glmS* ribozyme. Further consideration of phylogenetic data for the *glmS* ribozyme supports the existence of a 3$'$ pseudoknot by covariation of sequence within the loop of P3 and immediately downstream of P4 (16). As the P3 and P4 domains are known to enhance *glmS* ribozyme activity (5), the 3$'$ pseudoknot within this non-core region has thus been demonstrated to contribute to ribozyme folding and catalysis (17). The proposed P1.1 interaction, however, establishes a 5$'$ pseudoknot within the catalytic core of the *glmS* ribozyme, and is therefore expected to underpin core ribozyme folding and catalysis. Therefore, the putative pseudoknot organization of the catalytic core provides a refined model that will both support and require further scrutiny through biochemical analyses of ribozyme structure, GlcN6P binding and catalytic function.

## REFERENCES

1. Nudler,E. and Mironov,A.S. (2004) The riboswitch control of bacterial metabolism. *Trends. Biochem. Sci.*, **29**, 11–17.
2. Winkler,W.C. and Breaker,R.R. (2005) Regulation of bacterial gene expression by riboswitches. *Annu. Rev. Microbiol.*, **59**, 487–517.
3. Corbino,K.A., Barrick,J.E., Lim,J., Welz,R., Tucker,B.J., Puskarz,I., Mandal,M., Rudnick,N.D. and Breaker,R.R. (2005) Evidence for a second class of *S*-adenosylmethionine riboswitches and other regulatory RNA motifs in alpha-proteobacteria. *Genome Biol.*, **6**, R70.
4. Sudarsan,N., Barrick,J.E. and Breaker,R.R. (2003) Metabolite-binding RNA domains are present in the genes of eukaryotes. *RNA*, **9**, 644–647.

5. Winkler,W.C., Nahvi,A., Roth,A., Collins,J.A. and Breaker,R.R. (2004) Control of gene expression by a natural metabolite-responsive ribozyme. *Nature*, **428**, 281–286.

6. Barrick,J.E., Corbino,K.A., Winkler,W.C., Nahvi,A., Mandal,M., Collins,J., Lee,M., Roth,A., Sudarsan,N., Jona,I. *et al.* (2004) New RNA motifs suggest an expanded scope for riboswitches in bacterial genetic control. *Proc. Natl Acad. Sci. USA*, **101**, 6421–6426.

7. Doherty,E.A. and Doudna,J.A. (2000) Ribozyme structures and mechanisms. *Annu. Rev. Biochem.*, **69**, 597–615.

8. Fedor,M.J. and Williamson,J.R. (2005) The catalytic diversity of RNAs. *Nature Rev. Mol. Cell Biol.*, **6**, 399–412.

9. McCarthy,T.J., Plog,M.A., Floy,S.A., Jansen,J.A., Soukup,J.K. and Soukup,G.A. (2005) Ligand requirements for *glmS* ribozyme self-cleavage. *Chem. Biol.*, **12**, 1221–1226.

10. Xue,Y., Xu,Y., Liu,Y., Ma,Y. and Zhou,P. (2001) *Thermoanaerobacter tengcongensis* sp. nov., a novel anaerobic, saccharolytic, thermophilic bacterium isolated from a hot spring in Tengcong, China. *Int. J. Syst. Evol. Microbiol.*, **51**, 1335–1341.

11. Bao,Q., Tian,Y., Li,W., Xu,Z., Xuan,Z., Hu,S., Dong,W., Yang,J., Chen,Y., Xue,Y. *et al.* (2002) A complete sequence of the *T.tengcongensis* genome. *Genome Res.*, **12**, 689–700.

12. Morse,S.E. and Draper,D.E. (1995) Purine–purine mismatches in RNA helices: evidence for protonated G.A pairs and next-nearest neighbor effects. *Nucleic Acids Res.*, **23**, 302–306.

13. Nagaswamy,U., Voss,N., Zhang,Z. and Fox,G.E. (2000) Database of non-canonical base pairs found in known RNA structures. *Nucleic Acids Res.*, **28**, 375–376.

14. Ortoleva-Donnelly,L., Szewczak,A.A., Gutell,R.R. and Strobel,S.A. (1998) The chemical basis of adenosine conservation throughout the *Tetrahymena* ribozyme. *RNA*, **4**, 498–519.

15. Adams,P.L., Stahley,M.R., Kosek,A.B., Wang,J. and Strobel,S.A. (2004) Crystal structure of a self-splicing group I intron with both exons. *Nature*, **430**, 45–50.

16. Tucker,B.J. and Breaker,R.R. (2005) Riboswitches as versatile gene control elements. *Curr. Opin. Struct. Biol.*, **15**, 342–348.

17. Wilkinson,S.R. and Been,M.D. (2005) A pseudoknot in the 3′ non-core region of the *glmS* ribozyme enhances self-cleavage activity. *RNA*, **11**, 1788–1794.